Time-Resolved X-Ray Diffraction Reveals Movement of F Helix of D96N Bacteriorhodopsin during M-MN Transition at Neutral pH

Toshihiko Oka,*† Naoto Yagi,‡ Fumio Tokunaga,* and Mikio Kataoka§

*Department of Earth and Space Science, Faculty of Science, Osaka University, Toyonaka, Osaka 560-0043, Japan; †RIKEN Harima Institute, Mikazuki, Sayo, Hyogo 679-5148, Japan; ‡Life & Environment Division, Japan Synchrotron Radiation Research Institute (JASRI), Mikazuki, Sayo, Hyogo 679-5198, Japan; and §Graduate School of Material Science, Nara Institute of Science and Technology, Ikoma, Nara 630-0101, Japan

ABSTRACT D96N bacteriorhodopsin has two photointermediates with the deprotonated Schiff base: the M and MN intermediates. We measure the time-resolved x-ray diffraction of the D96N purple membrane after flash photoexcitation (pH 7.0, 25°C). The data clearly show the M-MN transition during the D96N photocycle. Low-resolution projection maps of these states show that the F helix of the MN intermediate shifts from its original position and this shift is much larger than that of the M intermediate. This indicates that the F helix moves in the M-MN transition of the D96N bacteriorhodopsin photocycle. Moreover, the existence of the MN intermediate in the D96N photocycle under neutral pH indicates that the MN intermediate is not peculiar to the alkaline condition. It is notable that the structural transition of M-MN is independent of the protonation state of the Schiff base. Therefore, the F helix movement precedes reprotonation of the Schiff base in the bacteriorhodopsin photocycle. Our previous study showed that the M-MN transition is hydration-dependent and that the MN intermediate is more hydrated than the M intermediate. Considering this together with the present results, we conclude that the movement of the F helix causes hydration of the cytoplasmic side, which promotes the reprotonation of the Schiff base.

INTRODUCTION

Bacteriorhodopsin (BR) is a light-driven proton pump that transports protons from the cytoplasmic to the extracellular medium by using absorbed photon energy. Its photocycle is characterized in the J, K, L, M, N, and O states by their spectra in the visible range (Lozier et al., 1975), which reflect the environment of the chromophore. One of the most important steps in the proton pumping is the reprotonation process of the Schiff base from D96 in the M-N transition. In the M intermediate, BR has a deprotonated Schiff base. Because D96 is located in a hydrophobic environment, it has an unusually high pK and is protonated before photoreaction. Therefore, the pK of D96 should be lowered during the M-N transition to transfer a proton to the Schiff base.

D96N-BR has been studied intensively as a model system in structural studies by diffraction methods (Koch et al., 1991; Kamikubo et al., 1997; Luecke et al., 1999). The formation process of the M intermediate in D96N is identical to that in the wild type, which is characterized as the deprotonation of the Schiff base to D85. Because D96N lacks the proton donor to the Schiff base, the decay of the M intermediate is accomplished by the reprotonation of the Schiff base directly from the aqueous milieu. It has been shown that the yellowish state of D96N with a deprotonated Schiff base in the alkaline state (pH 10) takes an N-like protein conformation, which is called the MN intermediate (Sasaki et al., 1992). Hydration-dependent protein conformation change for D96N in the alkaline state (pH 10) has been revealed by x-ray diffraction (Kamikubo et al., 1997). According to that study, a partially hydrated D96N tends to accumulate the M intermediate, whereas the fully hydrated one prefers the MN intermediate. These results indicate that two types of yellowish intermediates with a deprotonated Schiff base are present in the D96N photocycle. It could be argued that the MN intermediate in the D96N photocycle is an ordinary intermediate similar to the N intermediate in the wild type. The hydration-dependent M-MN transition suggests that the structural transition brings water molecules into the cytoplasmic channel to lower the D96 pK. However, because this experiment has so far been carried out only under the photo-steady-state and alkaline condition, it is necessary to verify that the M-MN transition actually occurs under a physiological condition and that the MN intermediate is not a special intermediate observed only under the alkaline condition. Therefore, we measured the decay kinetics of the D96N photocycle by time resolved x-ray diffraction using its purple membranes.

Three-dimensional x-ray crystallography of BR has illustrated the detailed structures of the early photo-intermediate state (Edman et al., 1999; Royant et al., 2000) and M (Luecke et al., 1999b, 2000; Sass et al., 2000). The data from these studies clearly showed how residues move and the hydrogen network changes in these intermediate states. However, the movements of helices F and G are rather small in these crystal structures, whereas the electron densities of

Submitted October 22, 2001, and accepted for publication January 14, 2002.

Address reprint requests to Mikio Kataoka. Graduate School of Material Science, Nara Institute of Science and Technology, Ikoma, Nara 630-0101, Japan. Tel.: 81-743-72-6100; Fax: 81-743-72-6109; E-mail: kataoka@ms.aist-nara.ac.jp.

Toshihiko Oka's present address is Life and Environment Division, Japan Synchrotron Radiation Research Institute (JASRI), Mikazuki, Sayo, Hyogo 679-5198, Japan.

© 2002 by the Biophysical Society

0006-3495/02/05/2610/07 $2.00

the cytoplasmic region between F and G helices are blurred in the three-dimensional crystal structure of the M intermediate reported by Luecke et al. (1999b). This finding indicates that the region is highly disordered. On the other hand, diffraction experiments on the purple membranes (Koch et al., 1991; Subramaniam et al., 1993; Kamikubo et al., 1996; Subramaniam and Henderson, 2000) have revealed that these helices move largely in M or MN. One possible explanation for this is that the force constraint from the three-dimensional crystalline lattice suppresses substantial helix movement (Subramaniam and Henderson, 2000). Therefore, a structural study of the purple membrane under a physiological condition is still important because it would be effective in better understanding the proton pump mechanism. Furthermore, such an investigation would provide additional information on the crystallography.

Structural studies on photointermediates have been carried out by accumulating specific intermediates by chemical treatment, mutation, or quenching methods. However, a structural study conducted during an actual photocycle is needed to confirm that the equilibrium intermediate structures observed so far actually coincide with the kinetic intermediate structures. Moreover, this would be a powerful method for studying intermediate states that have not been observed by other methods. Third-generation synchrotron radiation sources can produce incident x-rays that have a high enough intensity for such an experiment. Furthermore, two-dimensional detectors with a high frame rate and high counting efficiency suitable for time-resolved experiments are now available. We have already shown the effectiveness of time-resolved x-ray diffraction measurements on the BR photocycle (Oka et al., 2000). In that study, we reported that two different conformations appear during the decay process of the wild-type BR. Because the decay process of D96N is different from that of the wild type, it is useful to apply time-resolved x-ray diffraction measurement to D96N. We measured the time-resolved x-ray diffraction of D96N-BR to analyze the M-MN transition at successive stages in the neutral condition.

MATERIALS AND METHODS

Samples

The cells that produce the D96N mutant BR (Ni et al., 1990; Needleman et al., 1991) were a kind gift from Dr. J. K. Lanyi. The D96N mutant BR was isolated as purple membrane sheets by the standard method (Oesterhelt and Stoeckenius, 1974) and suspended in a 10 mM HEPES buffer (pH 7.0). A 20-μL drop of suspension was dried on a piece of polyester sheet, and another drop was layered onto the resulting wet film. The layering procedure was repeated three times for the x-ray diffraction experiments and one time for the optical measurements. The film was incubated at 25°C at 95% relative humidity for 1 day.

Absorbance measurements

Flash-induced absorbance changes at 410 and 570 nm of the D96N BR were measured to confirm deprotonation and reprotonation of the Schiff base as follows. The sample was placed between a reference halogen lamp (Mega Light 100, Hoya-Schott, Tokyo) and a monochromator (SPG-120S, Shimadzu, Kyoto) with a photomultiplier (R928-09, Hamamatsu Photonics, Hamamatsu, Japan). An analog-to-digital converter card (REX5054, Ratoc System, Osaka) connected to a notebook computer (Toshiba, Tokyo) recorded the output signals. The samples were excited with a xenon flash lamp (SA200E, Eagle-Shoji, Kanagawa, Japan) with Toshiba Y50 and C50D filters ($500 < \lambda < 630$ nm). The temperature was maintained at 25°C. The time resolution was 10 ms. The one-half width of the flash duration was ~350 μs, which was sufficient to completely convert the unphotolyzed BR into the photolyzed state.

Time-resolved x-ray diffraction

Time-resolved x-ray diffraction experiments were carried out at the Riken Beamline I at SPring-8 (Fujisawa et al., 2000). X-ray diffraction patterns up to a Bragg spacing of 7 Å were recorded by a charge-coupled device camera (C4880-80-14A, Hamamatsu Photonics) coupled with a Hamamatsu Photonics 6-inch x-ray image intensifier (Amemiya et al., 1995; Fujisawa et al., 1999, 2000). Two hundred frames were recorded with a 122-ms time resolution. The temperature was maintained at 25°C. The samples were excited by a xenon flash lamp with Toshiba Y50 and C50D filters ($500 < \lambda < 630$ nm) at 2.44 s after the start of the diffraction measurement corresponding to the 21st time frame.

Data treatment

A series of the sequential two-dimensional ring diffraction patterns was averaged circularly to reduce them to a set of sequential one-dimensional patterns. Ten different data sets were averaged. The sequential one-dimensional diffraction patterns are equivalent to an $m \times n$ matrix. This matrix was analyzed with the singular value decomposition (SVD) method (Henry and Hofrichter, 1992) with weights of data (Oka et al., 2000). Three significant components were extracted from the SVD analysis (see Results). The V spectra of the three extracted components were fitted with double exponential functions to analyze the kinetics as

$$\begin{pmatrix} V_1 \\ V_2 \\ V_3 \end{pmatrix} = C \begin{pmatrix} 1 \\ \exp(-k_1 t) \\ \exp(-k_2 t) \end{pmatrix},$$

in which C is a 3×3 matrix. According to the time constants thus obtained, diffraction profiles of the decomposed components were reconstituted to calculate difference Fourier maps.

The intensity of each Bragg reflection was estimated by profile fitting with a Gaussian function. Difference Fourier maps were calculated using phases and intensity ratios for overlapping reflections derived from cryo-electron microscopy data (Henderson et al., 1990).

Reaction model

In the D96N photocycle, M and MN intermediates were observed (see Results). When the reaction model is assumed to be M $\xrightarrow{k_f}$ MN $\xrightarrow{k_s}$ BR, the observed structure factor is

$$\begin{aligned} F = {} & F_{\mathrm{BR}} \\ & + \left[MN_0 + \left(\frac{k_f}{k_f + k_s} \right) M_0 \right] (F_{\mathrm{MN}} - F_{\mathrm{BR}}) \exp(-k_s t), \\ & + M_0 \left[(F_{\mathrm{M}} - F_{\mathrm{MN}}) - \left(\frac{k_f}{k_f + k_s} \right) (F_{\mathrm{MN}} - F_{\mathrm{BR}}) \right] \\ & \times \exp(-k_f t) \end{aligned}$$

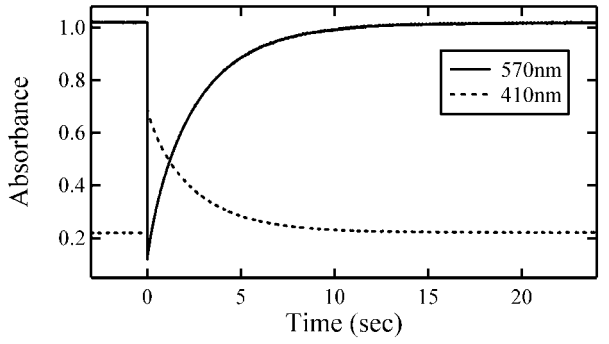

FIGURE 1 (*a*) Absorbance changes of D96N BR (pH 7.0, 25°C) at 570 and 410 nm before and after xenon flash lamp excitation. The sample was excited at time 0. Decays of 570 and 410 nm have almost the same time course because the intermediate states with the deprotonated Schiff base (M or MN intermediate, absorbance maximum 410 nm) are major components in this condition.

in which M_0 and MN_0 are the fraction concentrations of the M and MN intermediates at $t = 0$, and F_{BR}, F_M, and F_{MN} are the structure factors of the BR initial, M, and MN states. Therefore, the slow components are the differences of the MN and BR initial states. At $t = 0$, $F = F_{BR} + MN_0(F_{MN} - F_{BR}) + M_0(F_M - F_{BR})$. Hence, the difference at $t = 0$ is the sum of MN-BR and M-BR.

RESULTS

For the D96N mutant at pH 7.0, the life of the intermediate state with a deprotonated Schiff base is 100 times longer than that of the wild type. This is because D96N lacks the proton donor for the Schiff base (Miller and Oesterhelt, 1990). Fig. 1 shows the absorbance changes at 570 and 410 nm before and after flash excitation for D96N (pH 7.0, 25°C). The figure shows that the time course of 570 and 410 nm is almost the same. The absorption maximum of the BR initial state is at 570 nm, but the deprotonation of the Schiff base causes the absorbance maximum to shift to 410 nm. The kinetics is consistent with the findings of an earlier study (Miller and Oesterhelt, 1990) that showed a decay time of 2.4 s for D96N (pH 7.0, 10 mM ion, 20°C). Fourier-transform infrared clarified that the yellowish intermediate state of D96N possesses an N intermediate-like protein conformation, which is called the MN intermediate (Sasaki et al., 1992). Under our experimental conditions, the state after the flash excitation is regarded as a mixture of the M and MN intermediates.

Ten x-ray diffraction data of D96N (pH7.0, 25°C) were collected and added to improve the signal-to-noise ratio (Fig. 2). The time resolution of the measurement was 122 ms. Flash excitation was applied with a xenon flash lamp at the 21st frame in Fig. 2 to trigger the photocycle of D96N BR. Intensity changes due to the structural changes of BR during the photocycle were clearly observed. X-ray diffraction data was analyzed with the SVD to extract components in the decay process of the D96N photocycle. The results of

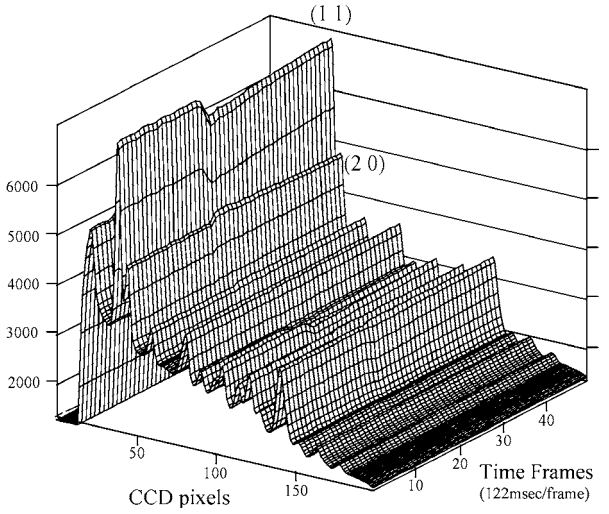

FIGURE 2 Time-resolved x-ray diffraction pattern of D96N BR (pH 7.0, 25°C) before and after xenon flash lamp excitation. Bragg peaks up to 7 Å are observed. Time resolution is 122 ms. Time frames are only shown up to the 50th frame, but diffraction patterns were recorded to the 200th frame. BR was illuminated at the 21st frame. Excitation causes changes in the diffraction pattern. These changes are due to structural changes in BR in its photocycle.

the SVD analysis are shown in Figs. 3 and 4. Only three major components are shown. The V spectrum of the *n*th component, V_n, is the time course of the changes in the *n*th

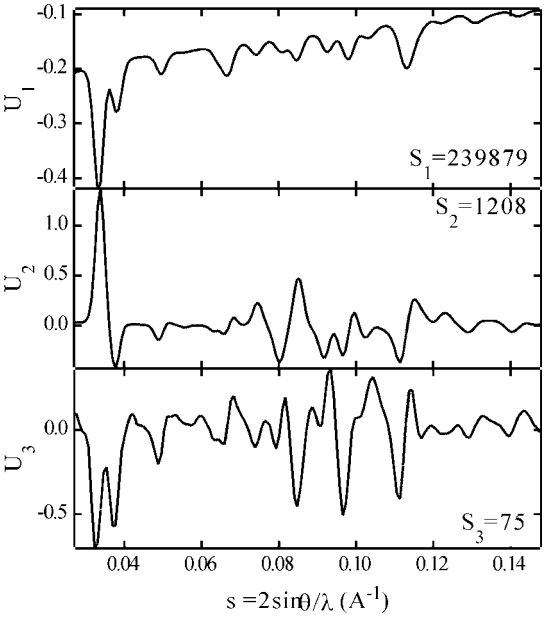

FIGURE 3 Time-resolved x-ray diffraction data of D96N (pH 7.0, 25°C) analyzed by SVD. Three major *U* spectra of D96N (pH 7.0, 25°C) are shown. Singular values of the higher components are 44, 28, 25, 24, 24, 23, 23, 22, and so on. Because the U_1, U_2, and U_3 of D96N are almost the same as those of the wild type (Oka et al., 2000), the structural changes in D96N and in the wild type are considered identical.

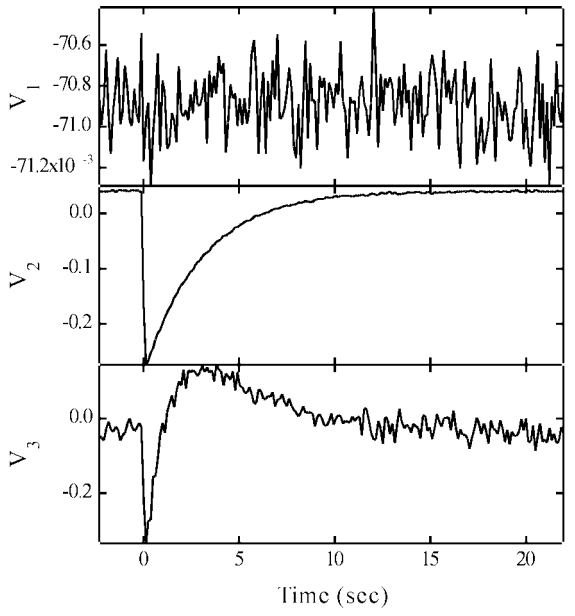

FIGURE 4 V spectra from the SVD analysis for weighted diffraction data of D96N (pH 7.0, 25°C). Because V_4 and V_5 do not have clear time dependency (data not shown), they are not distinguishable from noise. On the other hand, V_1, V_2, and V_3 have clear time dependence.

diffraction pattern, U_n. The nth singular value, S_n, is the magnitude of the nth component. The first component is significant because of its characteristic and distinct U spectrum and nonzero constant V spectrum. The diffraction pattern of U_1 is almost the same as that in Fig. 2 aside from its sign. The next two components are significant because of the distinct time dependences shown in their V spectra. Apparently, these changes are initiated by the flash excitation at time 0. The corresponding U spectra show nonrandom characteristic profiles. Therefore, the second and third components are derived from the structural changes in the BR photocycle. On the other hand, the V spectra of the fourth component and the higher components (data not shown) are independent of time and fluctuate around 0, indicating that these components are due to noise. Moreover, the first three singular values are larger than the other values, confirming that the first three components are signals and that the others are noise. The results of the SVD analysis suggest that the present data of the D96N photoreaction are composed of three components. In other words, D96N takes two different conformations during the decay process of the intermediate with a deprotonated Schiff base. Moreover, the first three U spectra of D96N are almost the same as those of the wild type observed for the M → N → BR reaction (Oka et al., 2000). This coincidence indicates that D96N also has two intermediate conformations similar to the M intermediate and N intermediate conformations of the wild-type BR.

Because the three components derived from the SVD analysis do not correspond directly to the three independent states in the photocycle, we must reconstitute the diffraction profiles for the three states from the three components. Therefore, we analyzed the kinetics of the three components. Three V spectra were fitted with double exponential functions to decompose to three conformational components depending on the decay rate. Table 1 shows the results of this fitting procedure. Because V_1 has no time dependency, double exponential functions were fitted to V_2 and V_3 (see Materials and Methods). Three components were reconstituted from these results: the time independent component B_0, slow decay component B_1 (rate constant k_1), and fast decay component B_2 (rate constant k_2). Fig. 5 shows three diffraction profiles obtained after reconstitution. Profile B_0 corresponds to a base diffraction profile of the BR initial state, whereas profiles B_1 and B_2 are diffraction profiles showing the difference from B_0 of two different

TABLE 1 Three V spectra (Fig. 4) were fitted by double exponential functions to decompose to three species depending on the decay rate

	B_0 constant	B_1 $k_1 = 0.3434 \pm 0.0021$	B_2 $k_2 = 0.657 \pm 0.020$
V_1	-0.070888 ± 0.000011		
V_2	0.04068 ± 0.00011	-0.3480 ± 0.0039	0.0166 ± 0.0042
V_3	-0.0343 ± 0.0015	1.000 ± 0.055	-1.373 ± 0.051

Because V_1 has no time dependency, double exponential functions were fitted to V_2 and V_3. Three components were reconstituted from this result: time independent component B_0, slow decay component B_1 (rate constant k_1), and fast decay component B_2 (rate constant k_2).

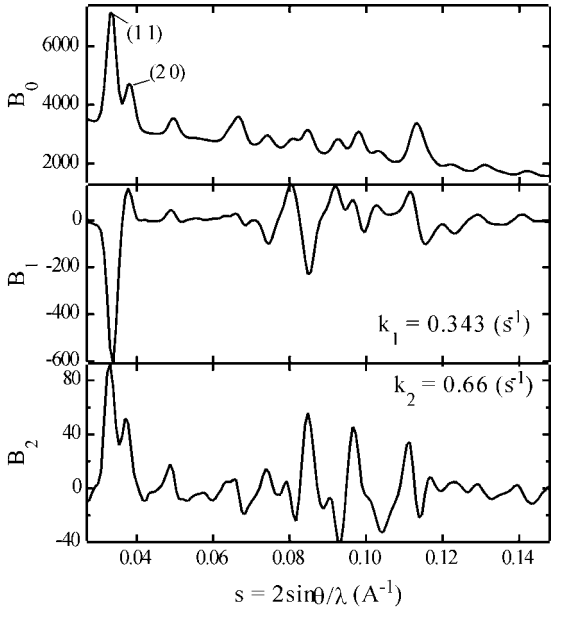

FIGURE 5 Reconstituted B spectra of weighted diffraction data (D96N, pH 7.0, 25°C). B_0 is a diffraction profile of the purple membrane of the BR initial state. B_1 is a slow decay component and B_2 is a fast one. The Schiff base of the D96N photo-intermediate observed under this condition is nearly deprotonated.

components that decayed with different time constants after the flash excitation. Profile B_1 is the intensity difference of the MN intermediate and BR initial states (MN-BR) (see Material and Methods). The ratio between the intensities of the (1 1) peak and the (2 0) peak is 6:1. On the other hand, the summation of profiles B_1 and B_2 is the sum of M-BR and MN-BR. The ratio of the summed (1 1) negative peak to that of the summed (2 0) positive peak is ~5:2. The intensity ratio of (1 1) to (2 0) is used as a criterion to distinguish the M from the N conformations (Kamikubo et al., 1997). The intensity of (2 0) is very small compared with the (1 1) intensity for the M conformation, whereas the ratio is close to 1 for the N conformation. The present time-resolved experiment reveals that at least two distinct conformations exist in the photocycle of D96N. The structural properties of these two components are close to the M intermediate conformation and the MN intermediate conformation in the photo-steady experiment (Kamikubo et al., 1997). Because the photointermediate of D96N has mainly a deprotonated Schiff base in the present time region (Fig. 1), the observed structural transition is from the M intermediate to the MN intermediate.

We analyzed these intensity profiles by the difference Fourier method and estimated the parts of the molecule that showed large changes. In this analysis, we used reflections up to a (5 1) reflection corresponding to a 10-Å resolution. Fig. 6 shows the difference electron density maps of the fast (Fig. 6 *b*) and slow (Fig. 6 *a*) components of D96N. The map of the slow component (Fig. 6 *a*) is the difference electron density map between the MN intermediate and the BR initial states (see Materials and Methods). This map is almost the same as that of the slow component of the wild type (Oka et al., 2000), which corresponds to the N intermediate. A large peak is observed on the F helix. On the other hand, a negative peak and a positive peak are observed on the F helix in the map of the fast component (Fig. 6 *b*). This result is interpreted as follows. The positive peak of the F helix is low just after the flash excitation (the summation map of the slow and fast components). It then increases as the fast component decays (the map of the slow component). On the other hand, the positive peak on the G helix (Fig. 6 *a*) is high but becomes low in the early stage of the decay process because the negative peak is observed at the same position in Fig. 6 *b*. This naturally implies that the electron density of the *F* helix increases in the transition from the M intermediate (M-type conformation) to the MN intermediate (N-type conformation) (Fig. 6). Therefore, the M-MN structural transition of D96N is considered the same as the M-N structural transition of the wild type in the helix movements (Oka et al., 2000).

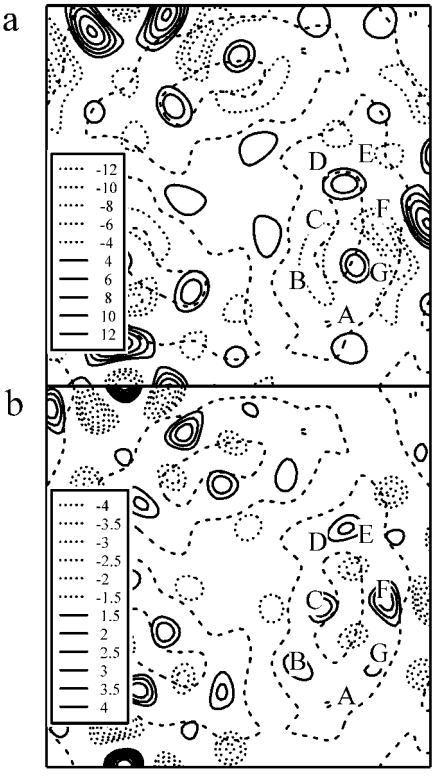

FIGURE 6 Difference Fourier maps of the slow and the fast decay components of D96N (pH 7.0, 25°C) B spectra in Fig. 5. (*a*) Map of the slow component. The BR structure near the F and G helices clearly changes. This difference map is almost the same as that of the N intermediate of the wild type. (*b*) Map of the fast component. A negative peak is seen outside the F helix. This position is the same as the positive peak of the F helix in *a*. Consequently, the difference density of the F helix is low just after flash excitation (the summation of the maps of the slow and fast components). It then increases as the fast component decays (map of the slow component). The positive peak heights of the F and G helices in *a* are 12.5 and 7.6, respectively. The negative peak height of the F helix in *b* is −3.7. The estimated errors of these maps are 1.8 and 0.54.

DISCUSSION

The present time-resolved x-ray diffraction of the D96N BR (pH 7.0, 25°C) revealed that two different conformations appear during the decay process of the intermediate state with a deprotonated Schiff base. Two independent components were reconstituted by SVD analysis. The structure of the slow component was close to that of the N intermediate. Because almost no N intermediate was observed for D96N under the neutral condition, the intermediate state we observed should be MN. Our findings from the present results are as follows. 1) The M-MN transition is directly observed by time-resolved x-ray diffraction of D96N. This indicates that the MN intermediate appears during the D96N photocycle at a neutral pH. 2) The transition is characterized as the movement of the F helix, which is the same structural change observed for the M-N transition in the wild type (Oka et al., 2000). 3) Our data also show that the BR changes its structure at the BR →M transition.

Rödig and Siebert (1999) reported that the MN intermediate was observed in the D96N BR photocycle under neutral pH. Their experimental condition (D96N, pH 7.0,

25°C) is similar to that of our present experiment. The existence of the MN intermediate in the D96N photocycle under neutral pH indicates that the MN intermediate is a common intermediate for the D96N photocycle but not peculiar to the alkaline condition.

The formation of the MN intermediate of D96N is a consequence of the movement of the F helix, as is the formation of the N intermediate for the wild type (Oka et al., 2000). The difference Fourier map (Fig. 6 *a*) shows that the electron density of the outside of the F helix increases during the transition, which indicates that a part of the F helix moved outward. The electron diffraction experiments reported so far have indicated that the cytoplasmic region of the F helix tilts away from the center of the molecule (Subramaniam et al., 1993; Vonck, 2000). Time-resolved electron paramagnetic resonance (EPR) experiments show that the E-F loop region also moves in the M-N transition (Thorgeirsson et al., 1997). The recent EPR studies show that the cytoplasmic end of the F helix rotates counterclockwise at the M-N transition as well as tilts outwards (Xiao et al., 2000; Rink et al., 2000). The structural change at the outside of the F helix and E-F loop region creates spaces in the cytoplasmic region of the BR and increases the accessibility of both the Schiff base and D96 to the cytoplasmic surface (Kataoka et al., 1994).

It is known that the hydration of the purple membrane affects the BR photocycle (Ferrand et al., 1993; Cao et al., 1991; Ganea et al., 1997). Highly hydrated BR (relative humidity 100% or 94%) accumulates the N intermediate in its photocycle, but less hydrated BR (relative humidity 85% or 75%) rarely does (Váró and Lanyi, 1991). A static x-ray experiment has shown that hydration of the BR also affects the M-MN structural transition of D96N under the alkaline condition (Kamikubo et al., 1997). Hydrated D96N prefers to take the MN intermediate, whereas the partially dehydrated one tends to become the M intermediate. The same effect is observed for the M-N transition of the wild type (Kamikubo and Kataoka, unpublished result). The observed hydration effect suggests that the movement of the F helix at the M-N transition is closely related to the change in the environment of D96 from hydrophobic to hydrophilic, because the pK of D96 decreases during the decay process of the M intermediate, whereas the M intermediate structure is more internal and less affected by surface-bound waters (Kamikubo et al., 1997).

The similarity between the M-MN transition of D96N and the M-N transition of the wild type suggests that the reprotonation of the Schiff base is not the cause of the structural change but a consequence of the structural change. EPR data support the conclusion that the F helix of BR changes just before the decay of the M intermediate (Rink et al., 2000; Mollaaghababa et al., 2000; Xiao et al., 2000). This indicates the existence of the MN intermediate state during the M-N transition of the wild-type BR photocycle. Combined with the hydration effect, the sequence of events of the proton transport is considered as follows: 1) the Shiff base is deprotonated and D96 is in a hydrophobic environment, remaining protonated (M intermediate); 2) the deprotonated Schiff base triggers the movement of the F helix to open the cytoplasmic side of the water channel (formation of the MN intermediate); 3) the rearrangement of water molecules at the cytoplasmic surface lowers the pK of D96, and D96 transfers its proton to the Schiff base (formation of the N intermediate).

X-ray protein crystallography is the only method available to directly inspect water molecules in the BR structure. Because the atomic structure of BR was resolved by x-ray diffraction of a crystal grown in the lipidic cubic phase in 1997 (Pebay-Peyroula et al., 1997), resolution of the BR atomic structure has been extended up to 1.55 Å (Luecke et al., 1999a). Crystal structures of photointermediates have also been revealed by the cryo-trapping method (Luecke et al., 1999b, 2000; Edman et al., 1999; Royant et al., 2000; Sass et al., 2000). The structure of D96N BR with the deprotonated Schiff base is considered to be the MN intermediate (Luecke et al., 1999b). The results showed the positions of water molecules in a proton conduction channel from the Schiff base to the extracellular region. However, cytoplasmic regions of the F and G helix were not clearly observed, probably because the structural change in the MN intermediate prevents all BR molecules from taking a uniform structure in the three-dimensional crystal. BR molecules are packed too tightly in the cytoplasmic regions of the F and G helix to take the MN intermediate structure. X-ray diffraction data shows that a heavy atom bound to I222C, which is located in the G helix, moves 2 Å toward the F helix in the MN intermediate state (Oka et al., 2000). Electron diffraction data on the F219L BR shows that the F helix, together with the E helix, tilts away from the center of the molecule, causing a shift of ~3 Å at the E-F loop in the N intermediate (Vonck, 2000). Subramaniam and Henderson (2000) also showed that the structural differences between the D96G, F171C, F219L triple mutant (with an N intermediate-like structure in the BR initial state), and the wild-type BR are mostly localized to the F and G helices. These changes inhibit all BR molecules from taking a uniform structure not only in a three-dimensional crystal but also in the purple membrane. The accumulation of the N intermediate in the photocycle depends on the excitation ratio of the BR (Tokaji, 1995). This photo-cooperative phenomenon is explained as follows. The movement of the F helix toward its neighbors in the crystal lattice is so large that it could not allow all molecules to change conformation simultaneously (Vonck, 2000). Therefore, it is necessary to circumvent these troublesome problems of helix movement to clarify how water molecules play a role in the proton pumping mechanism.

We thank Dr. Tetsuro Fujisawa (Riken Harima Institute) for his support for the x-ray diffraction measurement. This work was supported by the

SPring-8 Joint Research Promotion Scheme of Japan Science and Technology Corporation. Toshihiko Oka is grateful for the fellowships from the Japan Society for the Promotion of Science for Japanese Junior Scientists. The x-ray diffraction experiments were performed at SPring8 BL45XU Proposal Number 1999A0347.

REFERENCES

Amemiya, Y., K. Ito, N. Yagi, Y. Asano, K. Wakabayashi, T. Ueki, and T. Endo. 1995. Large-aperture TV detector with a beryllium-windowed image intensifier for x-ray diffraction. *Rev. Sci. Instrum.* 66:2290–2294.

Cao, Y., G. Váró, M. Chang, B. Ni, R. Needleman, and J. K. Lanyi. 1991. Water is required for proton transfer from aspartate-96 to the bacteriorhodopsin Schiff base. *Biochemistry.* 30:10972–10979.

Edman, K., P. Nollert, A. Royant, H. Belrhall, E. Pebay-Peyroula, J. Hadju, R. Neutze, and E. M. Landau. 1999. High-resolution X-ray structure of an early intermediate in the bacteriorhodopsin photocycle. *Nature.* 401: 822–826.

Ferrand. M., A. J. Dianoux, W. Petry, and G. Zaccai. 1993. Thermal motions and function of bacteriorhodopsin in purple membranes: effects of temperature and hydration studied by neutron scattering. *Proc. Natl. Acad. Sci. U. S. A.* 90:9668–9672.

Fujisawa, T., Y. Inoko, and N. Yagi. 1999. The use of a Hamamatsu X-ray image intensifier with a cooled CCD as a solution X-ray scattering detector. *J. Synchrotron Rad.* 6:1106–1114.

Fujisawa, T., K. Inoue, T. Oka, H. Iwamoto, T. Uruga, T. Kumasaka, Y. Inoko, N. Yagi, M. Yamamoto, and T. Ueki. 2000. Small-angle X-ray scattering station at the SPring-8 RIKEN beamline. *J. Appl. Crystogr.* 33:797–800.

Ganea, C., C. Gergely, K. Ludmann, and G. Váró. 1997. The role of water in the extracellular half channel of bacteriorhodopsin. *Biophys. J.* 73: 2718–2725.

Henderson, R., J. Baldwin, T. A. Ceska, F. Zemlin, E. Beckmann, and K. H. Downing. 1990. Model for the structure of bacteriorhodopsin based on high-resolution electron cryo-microscopy. *J. Mol. Biol.* 213: 899–929.

Henry, E. R., and J. Horfrichter. 1992. Singular value decomposition: application to analysis of experimental data. *Methods Enzymol.* 210: 129–192.

Kamikubo, H., M. Kataoka, G. Váró, T. Oka, F. Tokunaga, R. Needleman, and J. K. Lanyi. 1996. Structure of the N intermediate of bacteriorhodopsin revealed by X-ray diffraction. *Proc. Natl. Acad. Sci. U. S. A.* 93:1386–1390.

Kamikubo, H., T. Oka, Y. Imamoto, F. Tokunaga, J. K. Lanyi, and M. Kataoka. 1997. The last phase of the reprotonation switch in bacteriorhodopsin: the transition between the M-type and the N-type protein conformation depends on hydration. *Biochemistry.* 36: 12282–12287.

Kataoka, M., H. Kamikubo, F. Tokunaga, L. S. Brown, Y. Yamazaki, A. Maeda, M. Sheves, R. Needleman, and J. K. Lanyi. 1994. Energy coupling in an ion pump: the reprotonation switch of bacteriorhodopsin. *J. Mol. Biol.* 243:621–638.

Koch, M. H., N. A. Dencher, D. Oesterhelt, H. -J. Plöhn, G. Rapp, and G. Büldt. 1991. Time-resolved X-ray diffraction study of structural changes associated with the photocycle of bacteriorhodopsin. *EMBO J.* 10: 521–526.

Lozier, R. H., R. A. Bogomolni, and W. Stockenius. 1975. Bacteriorhodopsin: a light-driven proton pump in Halobacterium Halobium. *Biophys. J.* 15:955–962.

Luecke, H., B. Schobert, J. -P. Cartiller, H. -T. Richter, A. Rosengarth, R. Needleman, and J. K. Lanyi. 2000. Coupling photoisomerization of retinal to directional transport in bacteriorhodopsin. *J. Mol. Biol.* 300: 1237–1255.

Luecke, H., B. Schobert, H. -T. Richter, J. -P. Cartailler, and J. K. Lanyi. 1999a. Structure of bacteriorhodopsin at 1.55 A resolution. *J. Mol. Biol.* 291:899–911.

Luecke, H., B. Schobert, H. -T. Richter, J. -P. Cartailler, and J. K. Lanyi. 1999b. Structural changes in bacteriorhodopsin during ion transport at 2 angstrom resolution. *Science.* 286:255–260.

Miller, A., and D. Oesterhelt. 1990. Kinetic optimization of bacteriorhodopsin by aspartic acid 96 as an internal proton donor. *Biochem. Biophys. Acta.* 1020:57–64.

Mollaaghababa, R., H. -J. Steinhoff, W. L. Hubbel, and H. G. Khorana. 2000. Time-resolved site-directed spin-labeling studies of bacteriorhodopsin: loop-specific conformational changes in M. *Biochemistry.* 39:1120–1127.

Needleman, R., M. Chang, B. Ni, G. Váró, J. Fornes, S. H. White, and J. K. Lanyi. 1991. Properties of Asp212—-Asn bacteriorhodopsin suggest that Asp212 and Asp85 both participate in a counterion and proton acceptor complex near the Schiff base. *J. Biol. Chem.* 266: 11478–11484.

Ni, B. F., M. Chang, A. Duschl, J. K. Lanyi, and R. Needleman. 1990. An efficient system for the synthesis of bacteriorhodopsin in *Halobacterium halobium*. *Gene.* 90:169–172.

Oesterhelt, D., and W. Stoeckenius. 1974. Isolation of the cell membrane of *Halobacterium halobium* and its fractionation into red and purple membrane. *Methods Enzymol.* 31:667–678.

Oka, T., N. Yagi, T. Fujisawa, H. Kamikubo, F. Tokunaga, and M. Kataoka. 2000. Time-resolved x-ray diffraction reveals multiple conformations in the M-N transition of the bacteriorhodopsin photocycle. *Proc. Natl. Acad. Sci. U. S. A.* 97:14278–14282.

Pebay-Peyroula, E., G. Rummel, J. P. Rosenbusch, and E. M. Landau. 1997. X-ray structure of bacteriorhodopsin at 2.5 angstroms from microcrystals grown in lipidic cubic phases. *Science.* 277:1676–1681.

Rink, T., M. Pfeiffer, D. Oesterhelt, K. Gerwert, and H. -J. Steinhoff. 2000. Unraveling photoexcited conformational changes of bacteriorhodopsin by time resolved electron paramagnetic resonance spectroscopy. *Biophys. J.* 78:1519–1530.

Rödig, C., and F. Siebert. 1999. Distortion of the L→M transition in the photocycle of the bacteriorhodopsin mutant D96N: a time-resolved step-scan FTIR investigation. *FEBS Lett.* 445:14–18.

Royant, A., K. Edman, T. Ursby, E. Pebay-Peyroula, E. M. Landau, and R. Neutze. 2000. Helix deformation is coupled to vectorial proton transport in the photocycle of bacteriorhodopsin. *Nature.* 406:645–648.

Sasaki, J., Y. Shichida, J. K. Lanyi, and A. Maeda. 1992. Protein changes associated with reprotonation of the Schiff base in the photocycle of Asp96→Asn bacteriorhodopsin: the MN intermediate with unprotonated Schiff base but N-like protein structure. *J. Biol. Chem.* 267: 20782–20786.

Sass, H., J. G. Büldt, R. Gessenich, D. Hehn, D. Neff, R. Schlesineger, J. Berendzen, and P. Ormos. 2000. Structural alterations for proton translocation in the M state of wild-type bacteriorhodopsin. *Nature.* 406: 649–653.

Subramaniam, S., M. Gerstein, D. Oesterhelt, and R. Henderson, 1993. Electron diffraction analysis of structural changes in the photocycle of bacteriorhodopsin. *EMBO J.* 12:1–8.

Subramaniam, S., and R. Henderson. 2000. Molecular mechanism of vectorial proton translocation by bacteriorhodopsin. *Nature.* 406: 653–657.

Thorgeirsson, T. E., W. Xiao, L. S. Brown, R. Needleman, J. K. Lanyi, and Y. -K. Shin. 1997. Transient channel-opening in bacteriorhodopsin: an EPR study. *J. Mol. Biol.* 273:951–957.

Tokaji, Z. 1995. Cooperativity-regulated parallel pathways of the bacteriorhodopsin photocycle. *FEBS Lett.* 357:156–160.

Váró, G., and J. K. Lanyi. 1991. Distortions in the photocycle of bacteriorhodopsin at moderate dehydration. *Biophys. J.* 59:313–322.

Vonck, J. 2000. Structure of the bacteriorhodopsin mutant F219L N intermediate revealed by electron crystallography. *EMBO J.* 19:2152–2160.

Xiao, W., L. S. Brown, R. Needleman, J. K. Lanyi, and Y. -K. Shin. 2000. Light-induced rotation of a transmembrane alpha-helix in bacteriorhodopsin. *J. Mol. Biol.* 304:15–721.